Bioorganic & Medicinal Chemistry Letters 20 (2010) 3972–3976

Contents lists available at ScienceDirect

Bioorganic & Medicinal Chemistry Letters

journal homepage: www.elsevier.com/locate/bmcl

Structure based design of novel inhibitors for histidinol dehydrogenase from *Geotrichum candidum*

Sonia Pahwa [a], Simranjeet Kaur [a], Rahul Jain [b], Nilanjan Roy [a,*]

[a] Department of Biotechnology, National Institute of Pharmaceutical Education and Research, Sector 67, S.A.S. Nagar, Punjab 160062, India
[b] Department of Medicinal Chemistry, National Institute of Pharmaceutical Education and Research, Sector 67, S.A.S. Nagar, Punjab 160062, India

ARTICLE INFO

Article history:
Received 7 December 2009
Revised 25 March 2010
Accepted 27 April 2010
Available online 18 May 2010

Keywords:
Geotrichum candidum
Histidinol dehydrogenase
Homology modeling
Docking analysis
Antifungal compound

ABSTRACT

Histidinol dehydrogenase, the product of the HisD gene, mediates the final step in the histidine biosynthetic pathway. This enzyme has captured attention for drug discovery studies in past few years. Recently, our group cloned and expressed *Geotrichum candidum* histidinol dehydrogenase and successful screening of substrate analog inhibitors of histidinol dehydrogenase led to some antifungal compounds with IC_{50} values in micromolar range. In this study, we have done docking analysis of these antifungal agents in *G. candidum*. Two new compounds were designed based on the docking results and these compounds turned out to be potent inhibitors of *G. candidum* histidinol dehydrogenase, showing IC_{50} values as low as 3.17 μM.

The histidine biosynthesis pathway is an important pathway found in bacteria, fungi and plants.[1] One of the enzymes of this pathway, histidinol dehydrogenase (L-histidinol-NAD^+ oxidoreductase) is of particular interest as a target of antimicrobial agents.[2] Moreover, it is essential for virulence in various pathogens and plays an essential role in maintenance of infection.[3] Histidinol dehydrogenase (EC 1.1.1.23) (HDH) catalyses the terminal step in the biosynthesis of histidine, the four-electron oxidation of L-histidinol to histidine. HDH catalyzes the formation of L-histidine in two steps; NAD-dependent oxidation of L-histidinol to L-histindaldehyde, followed by another NAD-dependent oxidation to form L-histidine. This enzyme is a homodimeric zinc metalloenzyme with one Zn^{2+} binding site per monomer.[4,5] In bacteria HDH is a single chain polypeptide; in fungi it is the C-terminal domain of a multifunctional enzyme which catalyzes three different steps of histidine biosynthesis; and in plants it is expressed as nuclear encoded protein precursor which is exported to the chloroplast.[6]

Very few inhibitors of histidinol dehydrogenase been reported till date.[7–9] Dancer et al. reported the development of potential herbicides targeted against cabbage histidinol dehydrogenase.[9] Further, Abdo et al. reported the synthesis and biological activity of potential antibacterial compounds tested against histidinol dehydrogenase of *Brucella suis* cloned and expressed in *Escherichia coli*.[8] These substituted benzylic ketone derivatives derived from histidine can inhibit *Brucella* growth in minimal medium and abolish multiplication in human macrophages.[10]

Geotrichum candidum is an extremely common fungus with a world-wide distribution and is the causative agent of geotrichosis.[11,12] Pulmonary involvement is the most frequently reported form of the disease, but bronchial, oral, vaginal, cutaneous, and alimentary infections have also been reported.[13–15] In our previous studies, we have used a hybrid approach of screening substrate analog inhibitors of *G. candidum* histidinol dehydrogenase (GcHDH).[16] GcHDH has been cloned, expressed, an assay method developed for screening compounds and essential structures of antifungal compounds have been identified by quantitative structure–activity relationship (QSAR) analysis.[17] Based on our previously reported 3D QSAR studies, our aim was to design new active compounds starting from the docking analysis of imidazole derivatives reported in previous[16] and in this paper. In this study, docking of these substrate analog inhibitors of GcHDH was performed and results analyzed. Two new inhibitors were designed, synthesized and biologically evaluated as novel inhibitors of *G. candidum* histidinol dehydrogenase.

The molecular modeling studies of GcHDH were carried out on Windows XP platform using MOE (Molecular Operating Environment)[18] and SYBYL7.3[19] molecular modeling packages. Homology modeling module of the MOE was used for comparative protein modeling and molecular docking studies were performed using the FlexX program implemented in SYBYL7.3.

As a first step towards 3D structure prediction using homology modeling, the amino acid sequence of GcHDH (GenBank Accession

* Corresponding author. Tel.: +91 172 2214 687; fax: +91 172 2214 692.
E-mail address: nilanjanroy@nipeer.ac.in (N. Roy).

0960-894X/$ - see front matter © 2010 Elsevier Ltd. All rights reserved.
doi:10.1016/j.bmcl.2010.04.116

No. ABE73158) was obtained from the NCBI protein database. The HIS4 gene in *Saccharomyces cerevisiae* encodes a trifunctional protein,[20] which comprises the enzyme activities for AMP 1,6-cyclohydrolase (HIS4A), AMP-pyrophosphohydrolase (HIS4B), and histidinol dehydrogenase (HIS4C) and catalyzes three steps in the pathway of histidine biosynthesis. *G. candidum* HIS4 protein was also found to have HIS4A, HIS4B, and HIS4C subregions.[17] Amino acid sequence encoding HIS4C region (358–842) was selected based on sequence alignment with *S. cerevisiae* (Uniprot ID: P00815) and *Pichia pastoris* HIS4 protein (Uniprot ID: P45353). NCBI-BLAST (http://www.ncbi.nlm.nih.gov/BLAST)[21] was used to identify homologous structure for GcHDH by searching the structural database of protein sequences in the Protein Data Bank (PDB).[22] The BLAST search result picked up the crystal structure of *E. coli* L-histidinol dehydrogenase homodimer[23] (PDB ID: 1KAR) determined by Barbosa et al. with the sequence identity of 48% for GcHDH. 1KAR was then used as template for the homology modeling of both A and B chains of GcHDH protein. The final alignment of template with GcHDH was performed in needle program in EMBOSS.[24] The identity and similarity between the target and template was 43.5% and 55.5%, respectively (Fig. 1).

After the development of final best packing quality model for GcHDH, coordinates of Zn^{2+} and water molecule were added using MOE and optimized using an MMFF94 force field and PM3, a gradient 0.01 kcal/mol Å Hamiltonian, in MOE. For the reported homology model, coordinates of Zn^{2+} and water molecules in the active site were mimicked from the crystal structure of *E. coli* histidinol dehydrogenase. The catalytic Zn^{2+} cation in *E. coli* histidinol dehydrogenase is located at the bottom of the cavity occupied by the substrate histidinol and is octahedrally coordinated by Gln-259OE1, His-262NE2, Asp-360OD2, His-419BNE2, and two ligands from L-histidinol, ND1 and N.[23] The distances between the Zn^{2+} and residue atoms involved (Gln-311OE1, His-314NE2, Asp-414OD2, and His-473B-NE2) in zinc coordination in GcHDH are within the acceptable limits (Supplementary file 1 and Fig. 1). The RMS deviation of the GcHDH model chain A and chain B with chain A and chain B of the template *E. coli* histidinol dehydrogenase (1KAR), at the C-α region was calculated to be 0.867 and 0.827 Å, respectively, and in the backbone region 0.879 and 0.835 Å, respectively, and in the side chain region 1.976 and 1.803 Å, respectively.

The final model was refined by energy minimization to remove any steric clashes of the side chains with each other and/or with backbone atoms. The model was first subjected to a highly tethered

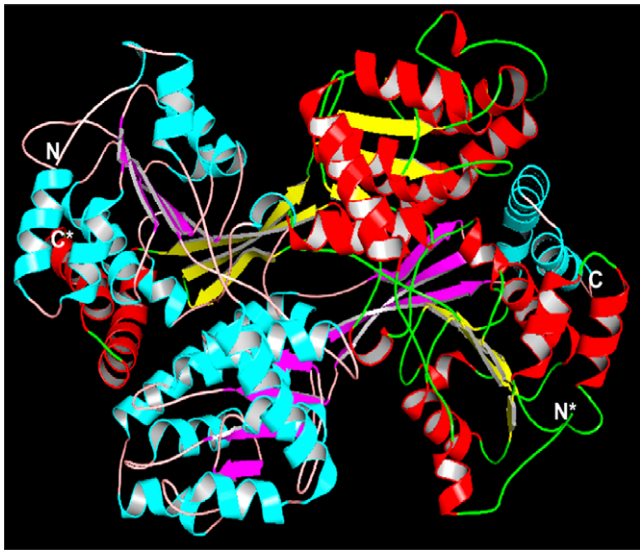

Figure 2. Structural topology of GcHDH homodimer. α Helices, β-strands and loops are colored cyan, magenta, and salmon, respectively, for chain A and in red, green and yellow, respectively, for chain B. The N- and C-terminal regions of chain A are denoted by N, C. For chain B, N- and C-terminal regions are denoted by N^* and C^*, respectively.

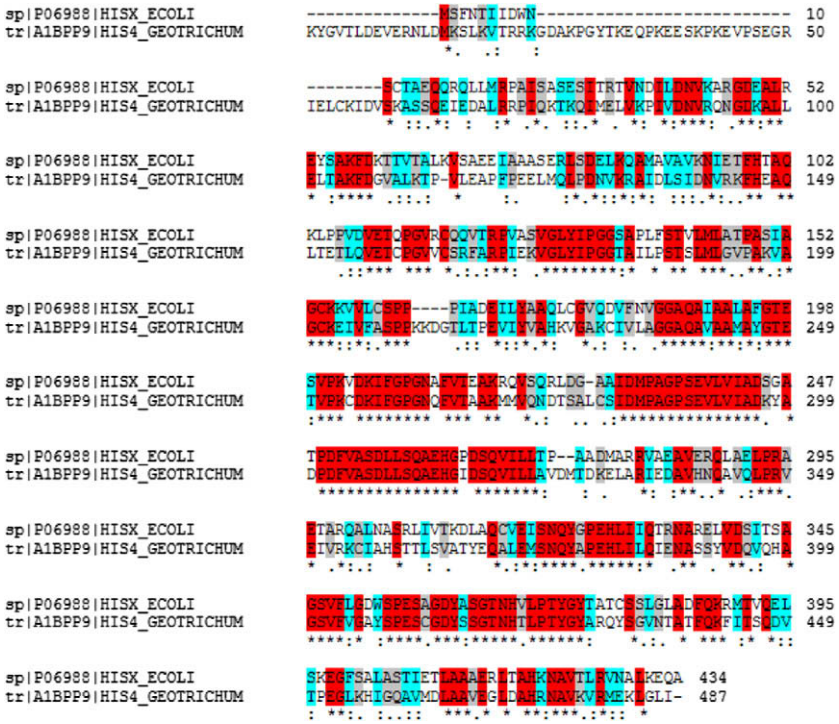

Figure 1. Sequence alignment of the GcHDH with *E. coli* L-histidinol (1KAR). Identical residues are highlighted in red and denoted by asterisk (∗). Highly conserved residues are denoted by double dots and colored cyan. Gray color depicts less conserved residues denoted by single dot. For GcHDH sequence, HIS4C region (358–844) was selected for alignment.

series of conjugate gradient minimization steps. The medium minimization options using Truncated Newton Optimization algorithm, with RMS gradient tests of 1 Å was used for GcHDH protein homodimer. For further refinement of the BsHDH and GcHDH model, the outlier residues were determined using Protein Geometry tool in MOE. Energy minimization of the selected outlier residues was carried out using AMBER94 force field with the RMS gradient of 0.05 Å. The stereochemistry and accuracy of the model was further gauged using Procheck[25] and Verify 3D[26,27] program in Structural Analysis and Verification Server (SAVES) (http://www.nihserver.mbi.ucla.edu/SAVES). The Ramachandran plot of GcHDH model obtained through Procheck showed 99.4% residues in the allowed region, 0.4% in the generously allowed region, and only 0.1% in the disallowed region (Supplementary file 1 and Fig. 2). This indicates that the backbone dihedral angles φ and ψ in the model were reasonably accurate. Verify 3D calculates 3D to 1D compatibility score and the graphical representation portrays the properly folded and misfolded regions in the protein structure by performing an Eisenberg analysis of the model (Supplementary file 1 and Fig. 3). From the above observations, the model was found sufficiently accurate for further structure-based analysis (Fig. 2).

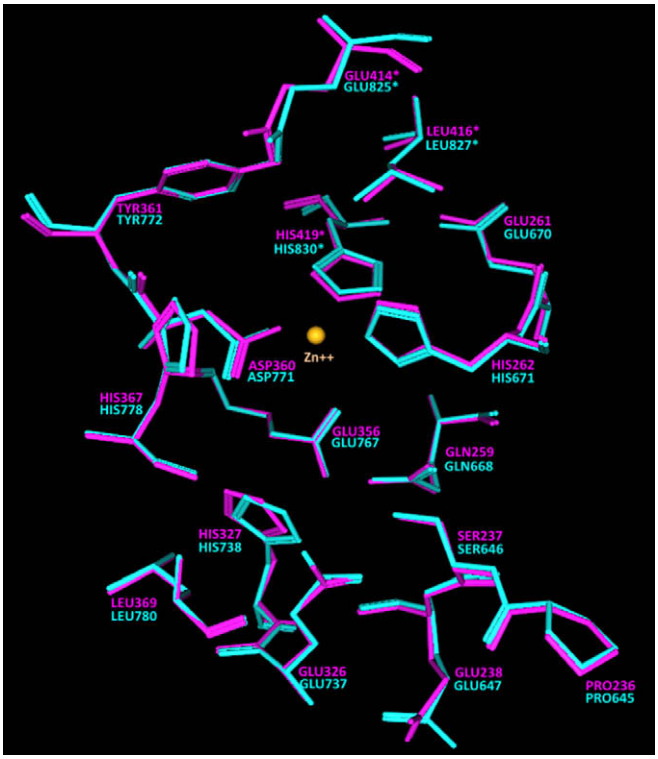

Figure 3. Active site residues of the template (purple) and GcHDH (cyan). Asterisk (*) denotes residues from B chain of respective enzymes.

To study the ligand–protein interactions in the active site of GcHDH, molecular docking was performed on the final refined homology model. Docking experiments were carried out using the FlexX module in SYBYL7.3 which utilizes the incremental construction algorithm. The binding site of substrate histidinol has already been defined for *E. coli* histidinol dehydrogenase.[23] Most of the active site residues of *E. coli* HDH superimposed well on GcHDH active site residues as observable from Figure 3. In order to validate our docking protocol, crystal structure of histidinol was extracted from *E. coli* histidinol dehydrogenase (PDB ID: 1KAE) and docked into the active site of GcHDH. A set of 30 conformations for histidinol was generated, from which one with the highest consensus score was selected. Once the docking protocol was validated, 6 imidazole derivative compounds were docked into the active site of GcHDH using same protocol. Compounds showing good activity from Class I and II were selected and docked into the

Table 1
Interaction of GcHDH active site residues

Mol. ID	Structure	Interacting residues		Total No. of H bonds	IC_{50} (μM)
		Chain A	Chain B		
Class I					
79	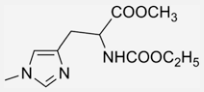	Ser646, His738, Leu780	–	9	29.3
92	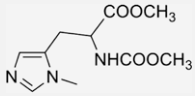	Thr545, Ser646, Glu737, His738, Gln668, Leu780	–	11	10.6
344	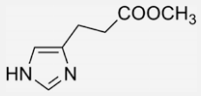	Gln668, His738, Ser646	Glu825	8	5.2
Class II					
334	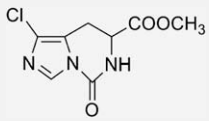	Ser646, Gln668, His671, His738, Glu737, Leu780	His830	10	122.2
333	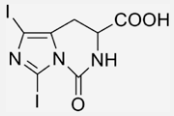	Thr545, Ser646, His738, Gln668, Glu767, Asp771	–	13	58.7
339	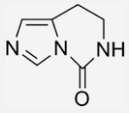	Leu780, His778	–	4	24.2

Table 2
Interaction and activity data for new designed compounds.

Mol. ID	Structure	Interacting residues		Total No. of H bonds	IC_{50} (μM)
		Chain A	Chain B		
S-3	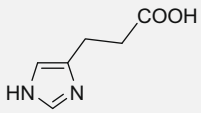	Gln668, Ser646, His738, His671, Asp771	His830, Glu825	13	3.17
RJ-278	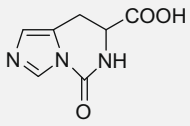	His671, Ser646, Gln668, His738, Glu737, Leu780	His830	15	3.56

active site of GcHDH homology model (Table 1). The activity of these compounds has been determined experimentally by our previous studies (reference). Based on the docking conformations and activity of these inhibitors, two novel inhibitors S-3 and RJ-278 were designed (Table 2) and docked in to the active site of GcHDH using same docking protocol and tested in vitro for their inhibitory activity against GcHDH.

The new compounds S-3 and RJ-238 were prepared as described in Supplementary file 2 and tested in enzyme and cell based assays according to previously reported procedures.[16]

The most active Class I compound 344 showed favorable conformations into GcHDH active site. The imidazole ring of 344 docked deep inside the cavity (Fig. 4A) and formed hydrogen bonding interaction with Glu825 and His738. Substitution of bulkier group at the α carbon decreases the inhibitory activity of the Class I molecules. Alkyl carbamate (–NHCOOR) substitution in compound 92 and 79 also decreases their activity. Compound 92 docked outside the cavity and its imidazole ring formed hydrogen bonding with Thr545 whereas, compound 79 formed no hydrogen bonding interaction with imidazole ring (Fig. 4B and C). Therefore it was assumed that imidazole ring should be less substituted and docked deep inside the cavity for better activity as steric hindrances due to *N*-methyl substituted imidazole causes a decrease in its activity. Based on the above observations, a new compound S-3 was designed in which the alkyl carbamate (–NHCOOR) substitution was detached and methyl group from the side chain was replaced by free –OH group. Docking of S-3 into the active site of GcHDH was performed, which showed imidazole ring situated deep inside the cavity and total 13 hydrogen bonding interactions with the receptor (Fig. 4D). The imidazole ring formed three hydrogen bonds inside the cavity. The compound S-3 was then tested for its inhibitory activity against GcHDH which showed an IC_{50} value of 3.17 μM (Table 2). This new compound resulted in a significant improvement in the inhibition of GcHDH.

Class II compounds docked in the outer cavity of the GcHDH active site (Fig. 5A–C). 339 compound formed hydrogen bonding interaction with Leu780 and His738. In 333 and 334, substitution of electronegative atom on the imidazole ring decreased the efficiency of imidazole ring for making hydrogen bonding interaction inside the cavity. Total 13 and 10 hydrogen bonds were observed for 333 and 334, respectively. Methyl substitution on side chain –COOH group reduces the hydrogen bonding interactions; therefore it can be assumed that free –OH of side chain carboxyl group is required for better activity. Based on these observations, another molecule RJ-278 was designed in which imidazole ring was kept unsubstituted and has a free carboxyl group on the side chain of

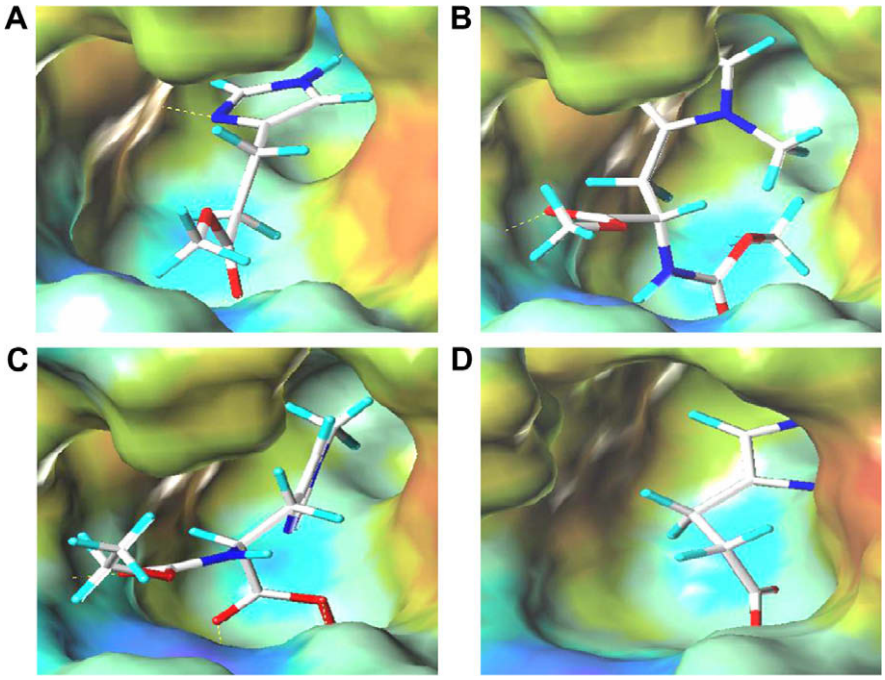

Figure 4. Selectively docked Class I compounds in GcHDH active site; 344(4A), 92(4B), 79(4C) and S-3(4D).

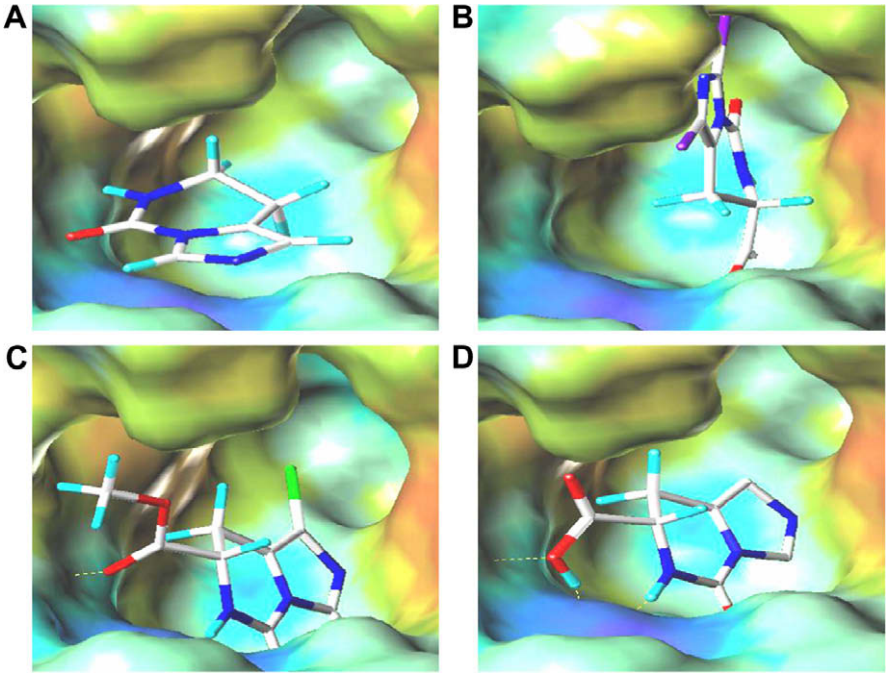

Figure 5. Selectively docked Class II compounds in GcHDH active site; 339(5A), 333(5B), 334(5C) and RJ-278(5D).

the molecule. As illustrated in Fig. 5D, RJ-278 docked well in the outer cavity of GcHDH active site and formed total fifteen hydrogen bonds. RJ-278 was then tested for biological activity, which showed IC_{50} value of 3.56 μM.

Our structural data are in agreement with the overall mechanism of action for HisD as proposed by Barbosa et al. where the residues Glu326 and His327 participate in acid–base catalysis.[23] From the crystal structure of *E. coli* histidinol dehydrogenase complexed with substrate, zinc and imidazole (PDB ID: 1KAE), it was observed that the hydroxyl group of substrate (L-histidinol) formed hydrogen bonds to the His367 and His327. The imidazole ring provided coordination to Zn^{2+} and also formed hydrogen bond to Glu414*. Similar interactions with corresponding residues in GcHDH were detected in S-3 and RJ-278 from our docking results. S-3 and RJ-278 made hydrogen bonds with above mentioned catalytically important residues, that is, His738, His778, Glu737, and Glu825 (His327, His367, Glu326, and Glu414 in *E. coli* HDH, respectively) (Fig. 3 and Table 2). These observations further validate our results and strengthen the proposed inhibition of GcHDH by S-3 and RJ-278.

In conclusion, histidinol dehydrogenase from *G. candidum* constitutes a suitable target for reported antifungal compounds, which represent valuable candidates for the potential development of novel inhibitors. 3D structure of GcHDH was determined using homology modeling technique. The docking studies show an extensive in silico evaluation of the substrate analog inhibitors of GcHDH for their potential antifungal activity. Moreover, the study of the interactions of the inhibitors with the active site of the HDH enzyme offered a better understanding of inhibitor action, allowing the design of new potential drug leads with improved inhibitory activity.

Supplementary data

Supplementary data associated with this article can be found, in the online version, at doi:10.1016/j.bmcl.2010.04.116.

References and notes

1. Alifano, P.; Fani, R.; Lio, P.; Lazcano, A.; Bazzicalupo, M.; Carlomagno, M. S.; Bruni, C. B. *Microbiol. Rev.* **1996**, *60*, 44.
2. Black, M. T.; Hodgson, J. E.; Knowles, D. J. C.; Riechard, R. W.; Nicholas, R. O.; Burnham, M. K. R.; Pratt, J. M.; Rosenberg, M.; Ward, J. M.; Lonetto, M. A. Google Patents, 2001.
3. Kishore, G. M.; Shah, D. M. *Annu. Rev. Biochem.* **1988**, *57*, 627.
4. Nagai, A.; Ohta, D. *J. Biochem.* **1994**, *115*, 22.
5. Grubmeyer, C.; Skiadopoulos, M.; Senior, A. E. *Arch. Biochem. Biophys.* **1989**, *272*, 311.
6. Nagai, A.; Ward, E.; Beck, J.; Tada, S.; Chang, J. Y.; Scheidegger, A.; Ryals, J. *Proc. Natl. Acad. Sci. U.S.A.* **1991**, *88*, 4133.
7. Kanaori, K.; Uodome, N.; Nagai, A.; Ohta, D.; Ogawa, A.; Iwasaki, G.; Nosaka, A. Y. *Biochemistry* **1996**, *35*, 5949.
8. Abdo, M. R.; Joseph, P.; Boigegrain, R. A.; Liautard, J. P.; Montero, J. L.; Köhler, S.; Winum, J. Y. *Bioorg. Med. Chem.* **2007**, *15*, 4427.
9. Dancer, J. E.; Ford, M. J.; Hamilton, K.; Kilkelly, M.; Lindell, S. D.; O'Mahony, M. J.; Saville-Stones, E. A. *Bioorg. Med. Chem. Lett.* **1996**, *6*, 2131.
10. Joseph, P.; Abdo, M. R.; Boigegrain, R. A.; Montero, J. L.; Winum, J. Y.; Kohler, S. *Antimicrob. Agents Chemother.* **2007**, *51*, 3752.
11. Buchta, V.; Otcenasek, M. *Mycoses* **1988**, *31*, 363.
12. Sfakianakis, A.; Krasagakis, K.; Stefanidou, M.; Maraki, S.; Koutsopoulos, A.; Kofteridis, D.; Samonis, G.; Tosca, A. *Med. Mycol.* **2007**, *45*, 81.
13. Jagirdar, J.; Geller, S. A.; Bottone, E. J. *Hum. Pathol.* **1981**, *12*, 668.
14. Kassamali, H.; Anaissie, E.; Ro, J.; Rolston, K.; Kantarjian, H.; Fainstein, V.; Bodey, G. P. *J. Clin. Microbiol.* **1987**, *25*, 1782.
15. Kantardjiev, T.; Kuzmanova, A.; Baikushev, R.; Zisova, L.; Velinov, T. *Folia Med.* **1998**, *40*, 42.
16. Pahwa, S.; Chavan, A. G.; Jain, R.; Roy, N. *Chem. Biol. Drug Des.* **2008**, *72*, 229.
17. Pahwa, S.; Roy, N. *Int. J. Integr. Biol.* **2008**, *3*, 1.
18. Chemical computing groups Inc.: Montreal, Canada.
19. Tripos Associates Inc., 1699. S. Hanley Rd., St. Louis, MO 631444, USA.
20. Keesey, J. K., Jr.; Bigelis, R.; Fink, G. R. *J. Biol. Chem.* **1979**, *254*, 7427.
21. Altschul, S. F. G. W.; Miller, W.; Myers, E. W.; Lipman, D. J. *J. Mol. Biol.* **1990**, *215*, 403.
22. Berman, H. M. W. J.; Feng, Z.; Gilliland, G.; Bhat, T. N.; Weissig, H.; Shindyalov, I. N.; Bourne, P. E. *Nucleic Acids Res.* **2000**, *28*, 235.
23. Barbosa, J. A.; Sivaraman, J.; Li, Y.; Larocque, R.; Matte, A.; Schrag, J. D.; Cygler, M. *Proc. Natl. Acad. Sci. U.S.A.* **2002**, *99*, 1859.
24. Needleman, S. B.; Wunsch, C. D. *J. Mol. Biol.* **1970**, *48*, 443.
25. Laskowski, R. M. M.; Moss, D.; Thornton, J. *J. Appl. Crystallogr.* **1993**, *26*, 283.
26. Bowie, J. U.; Luthy, R.; Eisenberg, D. *Science* **1991**, *253*, 164.
27. Luthy, R.; Bowie, J. U.; Eisenberg, D. *Nature* **1992**, *356*, 83.